

IV Interstellar Dust

Up until now we have been concerned primarily with physical properties in the gaseous phases of the ISM. We now turn our attention to a solid-state component: Interstellar Dust Grains.

Dust grains are solid, macroscopic particles composed of dielectric and refractory materials. As such, we have to deal with different and fundamentally less well-understood physics. Where before we have used quantum mechanics of atoms to explain the gas-phase spectra of neutral and ionized regions in the ISM, here we must consider macroscopic particles, and are largely dealing with the properties of solid bodies. Many of the physical details are empirical as we do not yet know the precise composition of dust grains, nor do we know their precise physical properties. Much of the physics we will discuss is based on tentative explanations of observed phenomena. Nobody has yet convincingly been able to produce grains in the laboratory, much less reproduce the conditions they would experience in interstellar space, although great progress is being made along these lines. Materials are known to change their properties under conditions of radiation bombardment (especially energetic particles like cosmic rays), and due to the inclusion of impurities. For example, we can measure the dielectric constants of pure water or CO₂ ices in the laboratory, but are unsure as to the degree we can rely upon those measurements for so-called “dirty ices” (those with embedded mineral impurities), or even pure ices that have been subjected to cosmic-ray bombardment in interstellar space.

The presence of dust grains in the ISM is deduced observationally in one of two basic ways:

I. Interaction with starlight:

We infer the presence of dust grains along a given line of sight by their effects upon starlight passing through them. These effects include:

1. Total and wavelength-selective extinction of starlight passing through dusty regions due to a combination of absorption and scattering.
2. Reflection of starlight by dusty clouds located behind bright stars (Reflection Nebulae).
3. Polarization of light either by scattering, or by passage through regions with macroscopically aligned non-spherical dust grains.
4. Absorption of starlight in Silicate bands, or various ice bands (e.g., H₂O and CO₂ ices).

II. Emission from dust grains:

Dust grains must also emit electromagnetic radiation that is directly detectable:

1. Thermal continuum emission from dust grains in radiative equilibrium with the local radiation field. This radiation emerges at mid- to far-IR wavelengths.
2. Thermal continuum emission from non-equilibrium heating of tiny grains emitted at near- to mid-IR wavelengths (1-25 μ m). These are also sometimes known as “Sellgren Grains”.
3. IR emission bands from heated grains. Many of these bands, however, are still not positively identified (or identified at all).

4. Radio continuum emission from rotating grains (both electric and magnetic dipole radiation). This has only recently been discovered as part of the Galactic radio background in recent years, and the explanations are compelling but still tentative.

We will be covering all of these topics with greater or lesser degrees of detail. Many are very active areas of research, and so only an introduction to the observational problem and the current state of understanding (or not) will be discussed.

How important is dust? In our Galaxy the gas-to-dust ratio is about 100:1. Since the ISM is about 10% of the baryonic mass of the Galaxy, dust grains comprise roughly 0.1% of the total. At the same time, they absorb roughly 30-50% of the starlight emitted by the Galaxy and re-radiate it as far-infrared continuum emission. This means that only 0.1% of the baryons are ultimately responsible for a third to a half of the bolometric luminosity of the Galaxy!

Dust grains are also the primary sites of molecular formation, and are thought to be responsible for essentially *all* of the H_2 in the ISM. Molecular chemistry is unthinkable without dust grains to act as reaction sites. Finally, the formation of planetary system is thought to begin when dust grains in a protostellar disk begin to coagulate into larger grains, leading to planetesimals and eventually to planets, carrying their complex organic molecules with them. Dust is not only the principle molecule builder, it might also be thought of as one of the principal ingredients of planetary formation, and life.

Dust matters.

Further Reading:

Two excellent recent reviews on interstellar dust are by Bruce Draine, the first an Annual Reviews article [2003, ARAA, 41, 241] and the second his Saas-Fee lectures, both from 2003. Both are available in PDF format from astro-ph ([astro-ph/0304489](https://arxiv.org/abs/astro-ph/0304489) and [astro-ph/0304488](https://arxiv.org/abs/astro-ph/0304488), respectively) and online. They cover the same material (he clearly used text and figures for both), but the Saas-Fee lectures go into a little more depth than the ARAA article. Both go beyond the basics covered here and are excellent resources for learning more.

IV-1 Interstellar Extinction

The manifestation of interstellar dust that first brought it to our attention is its ability to extinguish starlight passing through it. The most dramatic manifestations of interstellar dust are the dark clouds cataloged by E. E. Barnard at the beginning of the 20th century, many of which can be seen with the naked eye in the Milky Way.

The simplest case we can deal with is that of a distant star or other object behind a dusty region. In this case, the equation of radiative transfer can be solved simply in the pure-absorption case:

$$I_{\lambda} = I_{\lambda,0} e^{-\tau_{\lambda}}$$

Here $I_{\lambda,0}$ is the true spectrum of the source, I_{λ} is the observed spectrum, and τ_{λ} is the dust optical depth along the line of sight.

This form assumes that all of the extinction lines between the source and us (the so-called “dust-screen geometry”), and that there is no scattering of extraneous light into our line of sight (no source function in the transfer equation). The optical depth of the dust as a function of wavelength is parameterized in terms of an “Interstellar Extinction Curve”.

Classically, the interstellar extinction curve is measured by comparing the spectra of pairs of stars with identical spectral type (e.g., two B8 stars), one in the “clear” and the other extinguished by dust along the line of sight.

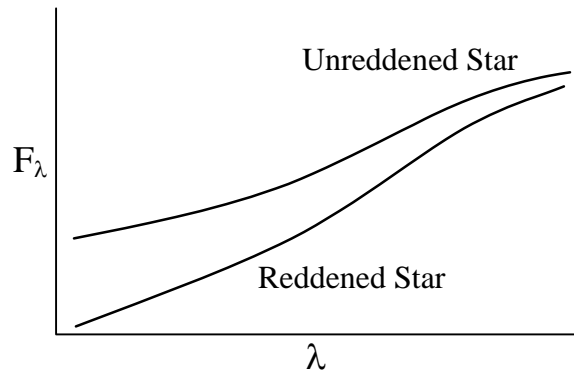


Figure IV-1: Effect of extinction on a stellar spectrum. Extinction is both a total diminution of the stellar light, and is wavelength-selective, in the sense that bluer wavelengths are more extinguished than red wavelengths.

It was quickly established that the interstellar extinction curve has a nearly universal form with wavelength along most sight lines, so that it is possible to write

$$\tau_{\lambda} = \text{const} \times f(\lambda)$$

The constant is a scaling factor parameterizing the amount of total extinction along the line of sight to a particular source, while the wavelength-selective extinction function, $f(\lambda)$, is universal (i.e., the same for all sources). The exact form of $f(\lambda)$ depends on the physics of the dust grains, and its near-universality suggests that the distribution of grain properties (composition and sizes) is similar everywhere. We will need to qualify what we mean by “universal”, however, as, Nature is not so simple, and interesting variations in the “universal” extinction law abound.

It is conventional at UV-to-NIR wavelengths to express the interstellar extinction curve in units of magnitudes, A_{λ} , normalized in terms of a **color excess** that represents the selective extinction:

$$E(B - V) = A_B - A_V$$

Here A_B is the absorption in magnitudes in the photometric B band ($\lambda_C \approx 4300\text{\AA}$), and A_V is the absorption in magnitudes in the V band ($\lambda_C \approx 5500\text{\AA}$). In general, extinction at a particular wavelength, A_λ , is the difference between the observed magnitude, m_λ , and the unabsorbed magnitude, $m_\lambda(0)$:

$$A_\lambda = m_\lambda - m_\lambda(0)$$

where:

$$m_\lambda = C_\lambda - 2.5 \log I_\lambda$$

Here C_λ is the magnitude zero-point, whose value is arbitrary and that depends on the details of the photometric system being used.

Since we are assuming simple absorption:

$$I_\lambda = I_{\lambda,0} e^{-\tau_\lambda}$$

The optical depth can be converted into a monochromatic extinction in magnitude units, A_λ :

$$A_\lambda = 2.5 \log(e) \times \tau_\lambda$$

$$A_\lambda \approx 1.086 \tau_\lambda$$

The standard interstellar extinction curve is normalized in terms of $E(B-V)$ as follows:

$$\frac{A_\lambda - A_V}{A_B - A_V} = \frac{E(\lambda - V)}{E(B - V)}$$

If the interstellar extinction curve has a universal form, then there will be a simple relation between the selective extinction, $E(B-V)$, and the total extinction at a specific wavelength, usually A_V or A_J . Conventionally, we define this in terms of the parameter R_V , **the ratio of total to selective extinction**:

$$R_V = \frac{A_V}{E(B - V)}$$

Observationally, R_V ranges between 2 and 6, but most often one finds the interstellar extinction law assumed by people as adopting one of two “typical” values for R_V :

$R_V=3.1$, typical of the Diffuse ISM.

$R_V=5$, typical of dense (molecular) clouds.

Beware: this division of interstellar dust into two characteristic values of R_V does not imply that R_V is bimodal! The larger “typical” value of R_V is thought to be a consequence of different distributions of grain sizes in high-density versus low-density environments, in the sense that larger R_V indicates larger grains on average. However, it could also be a consequence of differences in detailed grain properties, for example, the presence or absence of ice mantles. It is important to emphasize that R_V is an *empirical* factor introduced to account for observed differences in the “universal” extinction law seen in different environments. We do not yet fully understand the physics behind it.

R_V is a measure of the relative slope of the extinction curve, in the sense that larger values of R_V correspond to *flatter* extinction curves. In the limit $R_V \rightarrow \infty$, the extinction curve is completely flat, meaning that all wavelengths are absorbed equally and it is an ideal “gray” absorber. That the value is small (3–5) should tell you that interstellar dust is anything but gray.

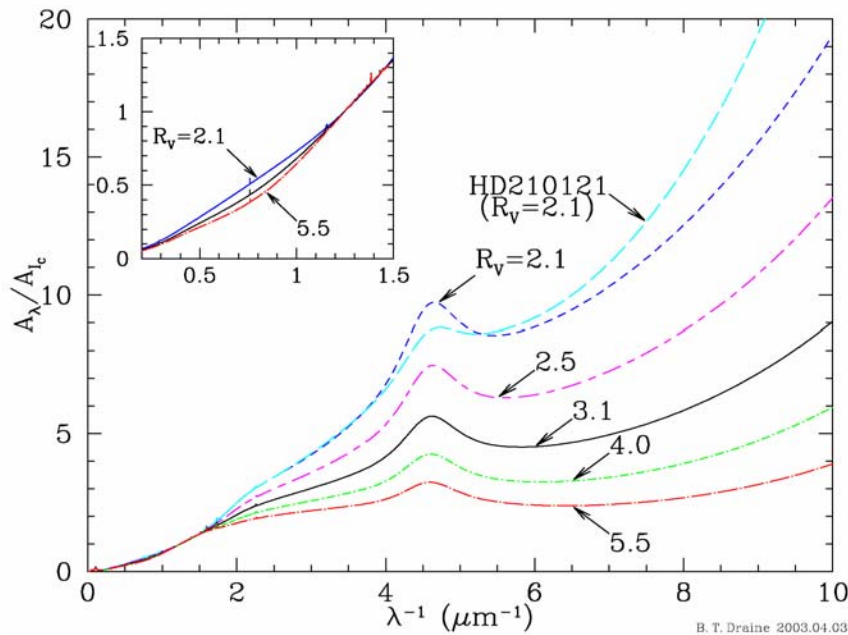
This simple one-parameter model for dust seems to hold reasonably well for wavelengths between $\sim 3000\text{\AA}$ and 7000\AA . Between $\sim 7000\text{\AA}$ and $\sim 8\mu\text{m}$, the extinction law is essentially independent of R_V . In the UV, however, there is considerable variation in the observed extinction, so much so that

multiple parameters are required to adequately fit it. The primary sources of variation are the strength, width, and central wavelength of the 2175Å bump feature (see below), and the slope and curvature of the UV continuous extinction for wavelengths less than ~3000Å.

The Interstellar Extinction Curve

At UV-to-NIR wavelengths the underlying interstellar extinction law is $A_\lambda \propto \lambda^{-1}$, with significant deviations at long and short wavelengths. While there are models of the interstellar extinction curve based on specific grain mixtures (see section IV-3), the standard interstellar extinction curve is determined empirically from spectroscopic measurements of obscured and unobscured sources. Recent tabulations of the UV/Visible/Near-IR extinction law are by Cardelli, Clayton, & Mathis [1989, ApJ, 345, 245], which has been nicely tabulated for $R_V=3.1$ and 5 by Mathis [1990, ARAA, 28, 37], and the general prescription described by Fitzpatrick [1999, PASP, 111, 63], shown below in a figure from Draine's 2003 review article

The reference interstellar extinction curves for these values of R_V are shown below, plotting A_λ normalized to A_{I_C} (Cousin's I) as a function of $1/\lambda$. The inset is an enlargement of the curve at infrared wavelengths. In the IR extinction is a smoothly varying function of wavelength until $\lambda \approx 10\mu\text{m}$, at which point the Silicate absorption band increases the extinction slightly. At shorter wavelengths ($\lambda < 1.2\mu\text{m}$), the extinction curves diverge for different R_V , with greater extinction for $R_V=3.1$. In the satellite UV, the strong “2175Å Bump” is the dominant feature, distorting the underlying approximately $1/\lambda$ shape.



Interstellar extinction curves for different R_V (from Draine 2003 ARAA)

In older papers you are likely to encounter other parameterizations of the interstellar extinction curve, such as Seaton [1979, MNRAS, 187, 73p] and Savage & Mathis [1979, ARAA, 17, 73]. While to a first approximation they all generally agree with one another, in detail this multiplicity of different parameterizations for the interstellar extinction law means that you must be very careful when combining extinction-corrected photometric data from different sources published at different times. A necessary exercise in such circumstances is to try to convert all of the data to a common extinction law. This is another reason why one should make a habit of publishing their raw uncorrected

photometry along with any extinction corrected values. Knowledge and fashions change, and providing the raw data makes the data proof against future revisions in the empirical extinction law.

Correlation of Extinction with the Total Hydrogen Column Density

The amount of visual extinction along a typical line of sight through the ISM is strongly correlated with the total column density of Hydrogen. Using both HI Ly α and H₂ Lyman-Werner bands in the UV (see Section V), Bohlin et al. [1978, ApJ, 224, 132] derived the current “standard” conversion between total visual extinction, A_V , and total Hydrogen column density, N_H , in the diffuse ISM:

$$A_V / N_H \approx 5.35 \times 10^{-22} \text{ mag cm}^2$$

for $R_V=3.1$. Fitzpatrick’s 1999 extinction measurements found

$$A_{I_c} / N_H \approx 2.96 \times 10^{-22} \text{ mag cm}^2$$

also for $R_V=3.1$, but now computing the total extinction in the Cousins I band ($\lambda_c=8000\text{\AA}$), which has become more common than A_V in modern parameterizations of the interstellar extinction curve.

This ratio is not universal, as shown by Rachford et al.’s [2002, ApJ, 577, 221] FUSE observations of 14 stars with lines-of-sight with $A_V>1$ through so-called “translucent clouds”. The extinction per unit total Hydrogen column density has been found to *increase* with larger R_V . An empirical fit good to ~10% gives this parameterization:

$$A_{I_c} / N_H = [2.96 - 3.55((3.1/R_V) - 1)] \times 10^{-22} \text{ mag cm}^2$$

In general, these values are very useful in practice. For example, if looking along diffuse ISM sight lines out of the Milky Way at extragalactic objects, one can use observations of the total HI column density along that line of sight, corrected for the estimated H₂ fraction, to estimate the amount of Galactic foreground extinction towards that object. Such estimates are provided by the NASA Extragalactic Database (NED) for all object queries, based on HI and dust maps compiled by Burstein & Heiles [1984, ApJS, 54, 33] and Schlegel, Finkbeiner, & Davis [1998, ApJ, 500, 525].

Alternatively, measurements of the extinction towards a particular Galactic source can be used to make a reasonable estimate of the total hydrogen column density along the line of sight, useful, for example, if you were planning observations at Far-UV or soft X-ray wavelengths.

Structure in the Interstellar Extinction Curve

In addition to the general continuous structure, the interstellar extinction curve has a lot of spectral “structure” in the form of absorption and emission by discrete components arising from the dust grains proper. They are extremely important as they give us vital clues as to the composition and structure of the dust grains.

The 2175 \AA Bump:

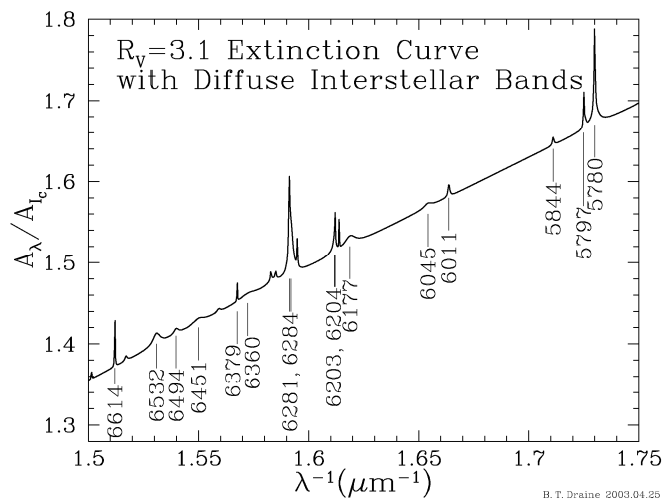
The strongest feature in the interstellar extinction curve is a broad “bump” centered at $\sim 2175 \pm 50\text{\AA}$ where there is additional absorption above the roughly λ^{-1} behavior at adjacent wavelengths. This is generally attributed to particles rich in carbon, either in the form of graphite, hydrogenated amorphous carbon grains, or various aromatic forms of carbon, but models have not yet succeeded in reproducing all of the details (like variations in the central wavelength and the width of the feature). It is notable that the feature is a strong function of the metallicity of the gas, with the UV bump appearing slightly weaker in the LMC extinction curve (metallicity ~50% solar), but essentially absent in the SMC extinction curve (metallicity ~10% solar). While there are many ideas, at present the carrier of the 2175 \AA feature is basically unidentified.

Mid-Infrared Silicate Features:

The strongest of these are a set of broad bands centered roughly at $9.7\mu\text{m}$ and $18\mu\text{m}$. The $9.7\mu\text{m}$ feature is associated with Si–O bending and stretching modes in Silicate minerals that generally arise around $10\mu\text{m}$, and so its identification is fairly secure. The fact that the $9.7\mu\text{m}$ band is fairly featureless, unlike what is seen in laboratory silicate crystals, suggests that this “astrophysical” silicate is primarily amorphous rather than crystalline in nature. The $18\mu\text{m}$ band is likely due to O–Si–O bending modes in silicates, and is also relatively securely identified. A band at $11.3\mu\text{m}$ has been tentatively identified with Si–C stretch/bend modes, and is usually seen in dust envelopes around Carbon stars. Because these compounds are attached to solid objects, the energy levels are distorted from the pure molecular bands seen in the laboratory, making exact one-to-one identification difficult.

Diffuse Interstellar Bands (DIBs):

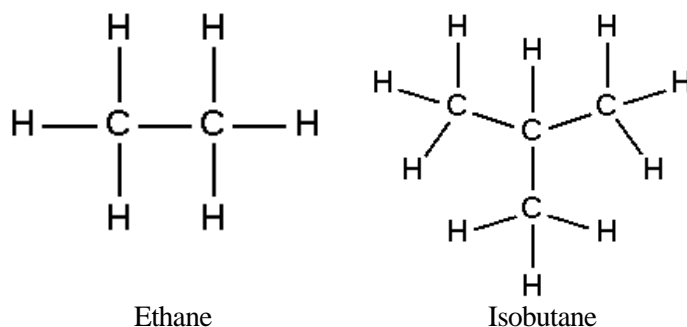
These are weak, very broad ($\text{FWHM} \geq 140\text{\AA}$) features seen at visible wavelengths. While discovered in 1922 by Heger, to date *none* of the many hundred DIBs have been securely identified (though provisional IDs abound). The fact that the bands are so broad rules out molecules with fewer than 5 atoms in the gas phase, so it is likely that the DIBs are associated with the dust grain population. The strongest DIB is at $\lambda 4430\text{\AA}$.



The strengths of DIBs are correlated with dust extinction, but the exact physical connection to dust grains is uncertain (i.e., we know DIBs and grains are related, but we cannot yet convincingly predict which DIBs will appear at what strengths from first principles). The identity and physics of the “carriers” of the DIBs is one of the outstanding mysteries of ISM research.

3.4 μm Aliphatic C–H feature:

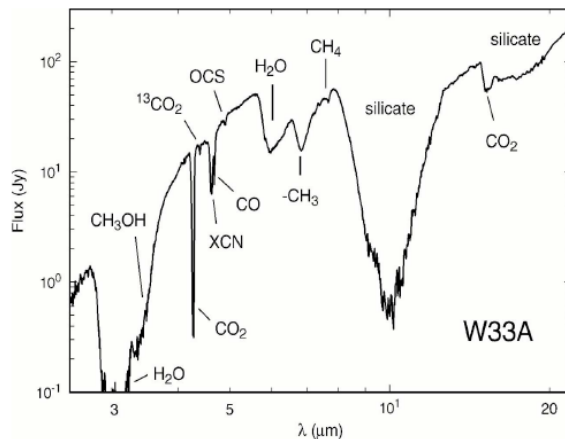
This is a broad extinction feature at $3.4\mu\text{m}$ seen along lines of sight where the interstellar extinction is very high ($A_V > 10$) associated with refractory grain material since it is often seen in regions of diffuse atomic gas. It is identified as a C–H stretching mode in “aliphatic” hydrocarbons (organic molecules with carbon atoms joined in straight or branched chains).



The origin of this feature is still unclear, but suggestions include aliphatic hydrocarbon residues produced by UV photolysis of ice mantles on grains, hydrogenated amorphous carbon, and hydrocarbon mantles on silicate grains.

Interstellar Ices:

The strongest ice feature is the $3.1\mu\text{m}$ O-H stretch band in water (H_2O) ice, two unidentified features at 6.1 and $6.8\mu\text{m}$, and a band at $15.2\mu\text{m}$ identified with CO_2 ice (see Whittet et al. 1996, A&A, 315, L375 and below). Other ice bands are CO , CH_4 , NH_3 , and CH_3OH . These are generally thought to arise in icy “mantles” that encase dust grains found in dense molecular clouds. Ice mantles are not found on grains in the general ISM, as exposure to the general interstellar radiation field sublimates the ices (for example, H_2O ice features in the Taurus dark cloud are only seen when $A_V > 3.3$). The ice bands are smeared out into broad features because they are in a solid state phase condensed onto a solid grain. An ice feature called XCN at $4.62\mu\text{m}$ is attributed to $\text{C}\equiv\text{N}$ bonds, but the “X” carrier is so far unidentified.

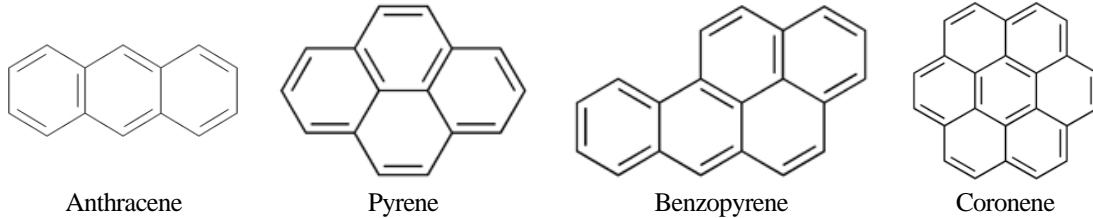


CO is a molecule most commonly observed in the gas phase (as we’ll see in the next chapter), but it can condense as a “frost” onto dust grains when the temperature drops below $\sim 17\text{K}$. Such condensation may lead to significant depletion of CO out of the gas phase deep inside molecular clouds. CO_2 has not yet been positively observed in the gas phase (despite numerous searches) but it *is* seen as an ice condensed onto grains surfaces. In both cases, the shape of the ice band depends on the presence of H_2O and the state of the molecules in the ice phase.

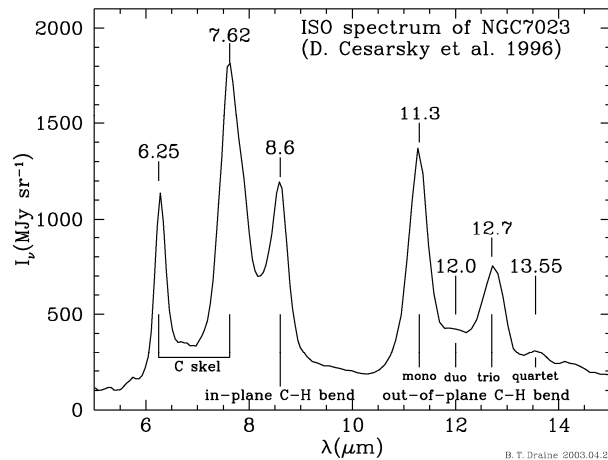
Polycyclic Aromatic Hydrocarbon (PAH) Features:

These are a family of five narrow emission bands at 3.3 , 6.2 , 7.7 , 8.6 , and $11.3\mu\text{m}$, sometimes with associated weaker features visible in bright sources, and underlying continua. Some (by now all?) have also been observed in absorption, particularly the $6.2\mu\text{m}$ feature. Previously

called the “Unidentified IR Bands” (or UIR bands in some older papers), they are now most often referred to generically as the “PAH features” because the most likely carriers appear to be polycyclic aromatic hydrocarbons. They are seen towards PNe, HII regions, reflection nebulae, and young stellar objects, primarily in dense regions. All of the PAH features have been observed in the diffuse ISM (see Mattila et al. 1996, A&A, 315, L353).



In aromatic carbon ring molecules the optically-active vibrational modes are various C-H and C-C bending and stretching modes which correspond reasonably well to the observed features. The 3.3 μ m feature is associated with C-H stretching, the 6.2 μ m and 7.7 μ m bands are C-C stretching modes, and the other bands are associated with various C-H in-plane and out-of-plane bending modes. Detailed association is difficult because laboratory PAHs are expected to differ from those found in interstellar space. Other suggestions for the carriers of these features are very tiny grains consisting of hydrogenated amorphous carbon (HACs) or carbonaceous composites (sometimes called QCCs, Q=Quenched), and solid carbon particles (“coal”).



PAH Emission features in the reflection nebula NGC7023 (5-15 μ m)

While they are associated with PAH molecules, no single particular PAH “carrier” has been positively identified for any of them. The matches between observations and laboratory spectra are always close, but never close enough. This has led some researchers to suspect that the PAH features arise from complex mixtures of different carriers (e.g., mixtures of neutral and positively-charged PAHs as discussed by Alamanola, Hudgins, & Sanford 1999 ApJ, 511, L115). Proposals include free PAH molecules, PAH “clusters”, and particles composed at least in part of PAHs. Other researchers have investigated what happens to the spectra of various PAHs, HACs, etc. when they are “damaged” or “modified” by the harsh radiation environment of interstellar space (e.g., ionization, addition or loss of hydrogen, etc.). Since such conditions cannot be easily reproduced in the laboratory (at least, nobody has succeeded yet), this is hard to test. Detailed quantum mechanical calculations are currently beyond our computational ability for such complex molecules. Further, the origin of the PAHs remains unknown and a matter of considerable speculation.

X-Ray Absorption Edges:

Dust grains can also absorb and scatter X-rays, although to an X-ray photon, a dust grain looks like a dense cloud of atomic gas, with the energies of the edges modified by being in solid materials rather than in the gas phase. Photoelectric absorption edges have been seen for C, O, Fe, Mg, and Si with Chandra and XMM.

Continuous Emission:

Two continuous emission components can arise from dust:

1. The “Extended Red Emission” (ERE), a broad featureless emission band peaking between $\sim\lambda 6100\text{\AA}$ and 8200\AA . In some nebulae this can contribute as much as 30–50% of the flux in the photometric I band (centered at $\sim\lambda 8800\text{\AA}$). It is almost certainly photoluminescence: absorption of a UV or optical photon followed by re-emission. In some nebulae the conversion efficiency can be as high as 10%. The most likely photoluminescent material is some kind of carbonaceous material, but no conclusive identification with a particular carrier (PAH, tiny silicate or carbonaceous grains, etc) has yet been made.
2. Thermal continuum radiation from dust grains. There are two forms:
 - a) FIR ($\lambda > 60\mu\text{m}$) continuum arising from warm normal-sized grains in thermal equilibrium with the ambient radiation field ($T_d \approx 20\text{--}40\text{ K}$). “Normal” size is $>0.01\mu\text{m}$ (100\AA). These include cooler “cirrus” emission (grains in equilibrium with the ISRF) and warmer dust associated with star clusters, esp. in star formation regions.
 - b) 3–30 μm continuum arising from non-equilibrium heating of tiny grains (sizes of 5–50 \AA) to temperature of a few hundred to a few thousand K.

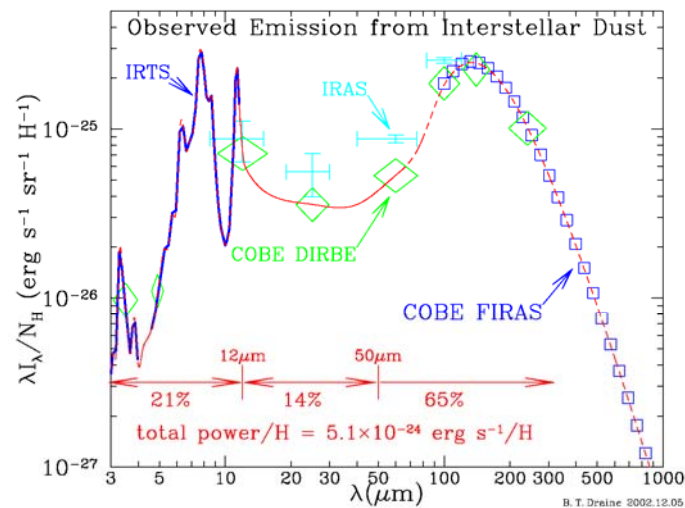


Figure 14: Observed emission from diffuse interstellar dust. Crosses: IRAS (Boulanger & Perault 1988); Squares: COBE-FIRAS (Finkbeiner et al. 1999); Diamonds: COBE-DIRBE (Arendt et al. 1998); Heavy Curve: IRTS (Onaka et al. 1996, Tanaka et al. 1996). The total power $\sim 5.1 \times 10^{-24} \text{ erg s}^{-1}/\text{H}$ is estimated from the interpolated broken line.

In general, the thermal emission is *not* well described by a blackbody radiation, but rather is a blackbody spectrum modified by a wavelength-dependent emissivity (λ^{-1} or λ^{-2}). We will discuss this in detail in section IV-5.

IV-2 Optical Properties of Dust Grains

Since we cannot (yet) make dust grains in the laboratory, we must rely on model calculations to explain their observed properties in interstellar space.

The important physics is the interaction between light and solid particles with specific dielectric or metallic properties (i.e., a real or complex index of refraction). This involves solving Maxwell's Equations for interactions with solid particles, the rigorous solutions of which (for homogeneous spherical particles) were worked out by Gustav Mie in 1908. The definitive treatment of Mie scattering for the case of interstellar dust grains was by van de Hulst (1957) in his book *Light Scattering by Small Particles*.

Basic Grain Parameters

Assume spherical dust grains with a radius a . We can define the following properties:

Geometric Cross-section

$$\sigma_G = \pi a^2$$

Effective Cross-section

$$\sigma \equiv \pi a^2 Q_{\text{ext}}(a, \lambda, \mu)$$

The latter defines the quantity Q_{ext} , the extinction efficiency of the dust grain.

The index of refraction, μ , has both real and imaginary parts:

$$\mu = n - in'$$

If the real part (n) is large, the grain is an effective *scatterer*, which is the case for dielectric grains or icy grains. If the imaginary part (n') is large, the grain is an effective *absorber*, e.g., as is the case for metallic grains.

It is convenient to parameterize the sizes of the grains in terms of the dimensionless size parameter

$$x \equiv \frac{2\pi a}{\lambda}$$

This relates the grain size to the wavelength of the incident light. Note that this is a completely classical treatment in which we shall treat light as electromagnetic waves instead of discrete photons. We will encounter semi-classical treatments (which consider the interactions of grains and photons) when considering non-equilibrium heating of tiny grains.

Grain Optical Depth and Albedo

The optical depth due to dust is the product of the grain column density and absorption cross-section:

$$\tau_\lambda = N_{\text{gr}} \sigma_{\text{gr}} Q_{\text{ext}}$$

Here N_{gr} is the column density of grains along the line of sight, σ_{gr} is the geometric cross-section of a dust grain, and Q_{ext} is the dimensionless extinction efficiency. In order to derive the observed interstellar extinction curve, A_λ , we need to know the distribution of grain sizes along the line of sight and the optical properties of the grains. The optical properties of the grain are all encapsulated within the relatively unassuming Q_{ext} term, which is a function of (at least) wavelength, grain size (a), and complex refractive index, μ . The real part of μ is the index of refraction, n , familiar from classical optics, whereas the imaginary part represents absorption or damping.

In general, Q_{ext} can be divided into scattering and absorption terms:

$$Q_{\text{ext}} = Q_{\text{scat}} + Q_{\text{abs}}$$

with the scattering part commonly expressed in terms of the **grain albedo**, ω :

$$\omega = \frac{Q_{\text{scat}}}{Q_{\text{ext}}}$$

An idealized pure-scattering grain would have $\omega=1$, whereas a pure absorbing grain would have $\omega=0$. There is an additional angular dependence to the scattering, in the sense that grains are strongly forward scattering. We will not treat this complicating factor here for simplicity, but keep it in mind as it is an important feature of detailed dust models as we'll see later.

For icy particles $Q_{\text{scat}} \gg Q_{\text{abs}}$, but $Q_{\text{abs}} \neq 0$. Thus even the most strongly scattering grains absorb some of the incident radiation and heat up. This means that they must then emit at least some thermal emission. There are two limiting cases of interest (see van de Hulst for a full rigorous treatment):

Long-Wavelength Case: small x ($a \ll \lambda$)

The long-wavelength limit is classical Rayleigh scattering. In the simplified case of dielectric spheres with no absorption (μ is real), we have

$$Q_{\text{ext}} \approx Q_{\text{scat}} = \frac{8}{3} x^4 \left| \frac{\mu^2 - 1}{\mu^2 + 2} \right|^2$$

Substituting in the definition of x , this reduces to

$$Q_{\text{scat}} \propto \lambda^{-4}$$

Short-Wavelength Case: large x ($a \gg \lambda$)

The short wavelength limit is classical Mie Scattering. Consider again the pure-scattering case, in the regime of $\mu \approx 1-2$. Here

$$Q_{\text{ext}} \approx Q_{\text{scat}} = 2 - \frac{4}{\rho} \sin \rho + \frac{4}{\rho^2} (1 - \cos \rho)$$

where

$$\rho = 2x(\mu - 1)$$

In this case, the behavior of Q_{ext} with x is oscillatory (sine and cosine terms). The maxima in Q_{ext} occur (roughly) when the twice-refracted light passing through the particle interferes constructively with the light diffracted *around* the particle. This is sketched in Figure IV-2.

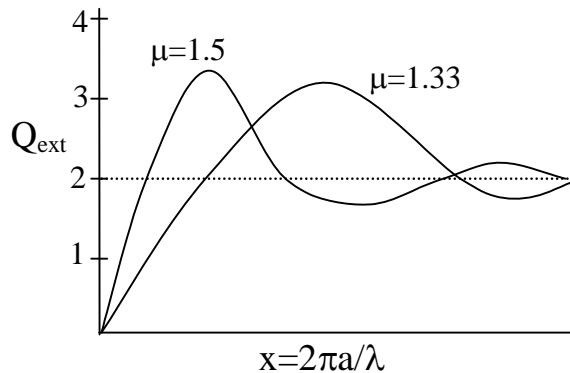


Figure IV-2: Plot of Q_{ext} versus x for materials with 2 different μ 's.

As x becomes very large $Q_{\text{ext}} \rightarrow 2$. This follows from Babinet's principle, which states that the diffraction pattern from an obstacle is the same as that from an aperture of the same cross-section (cf. any introductory optics text like Hecht & Zajac). In this limit the dust grain acts like a macroscopic, opaque spherical ball. The location of the first peak depends on the index of refraction roughly as $1/(\mu-1)$, and represents a resonance between the incident light and the dipole moment of the particle, hence the definition of ρ above.

A classical Mie scattering curve for a given grain size shows a sharp rise at long wavelengths (small x), and then flattens out at short wavelengths. The fact that the observed interstellar extinction curve is so broad tells us that there must be a distribution of particle sizes, and the relative flattening at short wavelengths suggest that there are more small grains than large grains in the ISM.

If we now allow the grain to have a finite absorption term (i.e., the imaginary part to the index of refraction is non-zero), at long wavelengths:

$$Q_{\text{abs}} > Q_{\text{scat}}$$

The absorption term is the imaginary part:

$$Q_{\text{abs}} = -4x \operatorname{Im} \left(\frac{\mu^2 - 1}{\mu^2 + 2} \right)$$

hence:

$$Q_{\text{abs}} \approx \lambda^{-1}$$

Recall that $Q_{\text{ext}} \propto \lambda^{-1}$ is approximately what is observed as the underlying interstellar extinction curve in the UV-to-NIR parts of the spectrum.

IV-3 The Physical Properties of Dust Grains

Grain Materials

Dust grains are expected to be composed of abundant refractory materials (primarily carbon, silicon, etc.) and compounds of Hydrogen and abundant gases like Oxygen. The grain composition determines the index of refraction needed to compute its optical properties. There is no one single type of “grain” that will suffice. Rather, a mixture of different types of grains formed under different physical conditions is required. The leading materials are silicates and carbonaceous (“carbon bearing”) materials, with ices of volatile compounds like water or CO₂ condensed on their surfaces (e.g., “ice mantles”). Pure metallic grains (e.g., iron spheres or needles) have also been considered. In general, silicates are expected to provide a substantial fraction of the total mass in dust grains in the ISM, followed by carbonaceous (carbon-bearing) compounds.

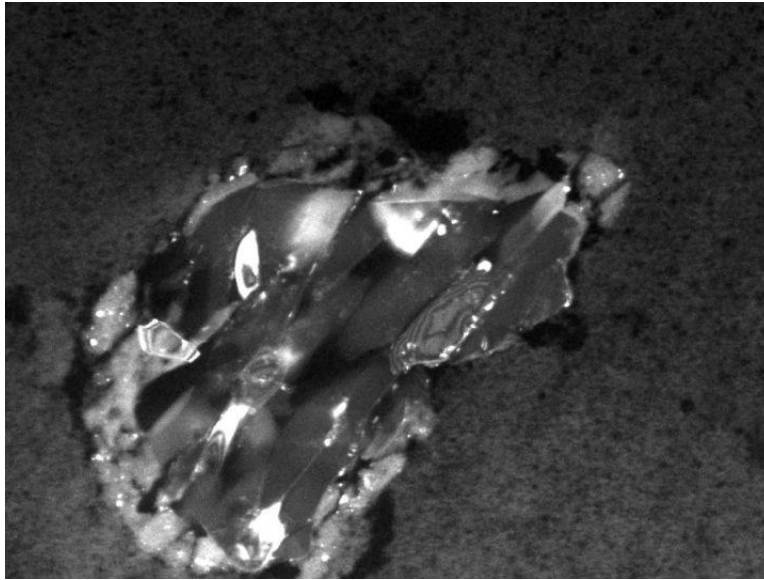
The indices of refraction of typical grain materials compared to an idealized perfectly reflecting spherical grain are as follows:

Perfectly Reflecting Spheres:	$\mu \rightarrow \infty$
“Pure” (non-absorbing) ices or pure silicates:	$\mu = 1.33$
“Dirty Ices” with absorbing “impurities”:	$\mu = 1.33 - 0.09i$
Metallic grains (e.g., iron spheres):	$\mu = 1.27 - 1.37i$

Note that the absorptive properties of a grain are parameterized by the imaginary part of the complex index of refraction. An overall extinction curve is derived using mixtures of grains of different types to try to reproduce the observed extinction curve.

The need for a complex index of refraction with an absorptive imaginary part can be understood from observations of familiar materials. Consider an ice cube made of pure water: it is transparent at visible wavelengths (ignoring bubbles or other imperfections). To make tiny ice particles act as interstellar absorbers at UV or Visible wavelengths you would need to pollute the ice to make it opaque, hence “dirty ices”. The impurities add an imaginary part to the complex index of refraction, as shown in the table above. Similarly, consider a pure quartz crystal (fused silica: SiO₂). High-purity fused silica is often used to make lenses in near-UV, visible, and near-IR instruments. Impurities in quartz can make it translucent or “milky” or it can give it a color. For example, Amethyst is a form of quartz that takes on a purple color because of contamination by small amounts of manganese (and a little iron) that contributes an imaginary component to its index of refraction.

This has led some researchers to propose a fictitious “interstellar silicate” with an imaginary index of refraction chosen specifically to reproduce the observed interstellar extinction curve. This is meant not to represent a particular real type of silicate grain, but instead to stand in for what is likely an ensemble of astrophysical silicates with different types and amounts of contamination, and mix of crystalline and amorphous forms (probably ~5% crystalline and 95% amorphous in the ISM, although different crystalline fractions have been suggested in other dusty environments like circumstellar dust shells). The crystalline silicates expected are those formed from compounds with Fe and Mg since both of these elements are astrophysically abundant. The principal forms expected are **Pyroxenes** (Mg_xFe_{1-x}SiO₃), which includes such minerals as Enstatite (MgSiO₃) and Ferrosilite (FeSiO₃), and **Olivines** (Mg_{2x}Fe_{2-2x}SiO₄), which includes such minerals as Fayalite (Fe₂SiO₄) and Forsterite (Mg₂SiO₄). All of these are common in meteorites, and spectral signatures of Enstatite and Forsterite have been seen in the dusty shells around AGB stars. Olivine and Forsterite have been seen in comets and in dust grains captured by the Stardust mission.



2 μ m grain of Forsterite captured by Stardust (NASA image)

Carbonaceous dust grains include pure carbon in both crystalline form (i.e., diamond and graphite), and amorphous or glassy form (i.e., composed of a mixture of graphite and diamonds), and hydrocarbons in the form of hydrogenated amorphous carbons, polycyclic aromatic hydrocarbons (PAHs), and aliphatic hydrocarbons. Also seen, but rare (probably less than 5% of all forms of carbonaceous grains), are other carbonaceous compounds like Silicon Carbide (SiC) and carbonates like Calcite (CaCO_3) and Dolomite ($\text{CaMg}(\text{CO}_3)_2$).

Grain Shapes

Spherical grains are usually considered because they permit straightforward analytic solutions. The reality, however, is that grains are not spheres. For example, the observed polarization of starlight passing through dust grains demands that the grains be non-spherical. Still, we can learn something about the basic mix of properties even if we continue to adopt the simple procedure of only considering spherical grains. The non-sphericity of the grains should enter as corrections to the predictions of spherical grain models.

The detailed grain shape, however, is an important consideration for working out grain dynamics (thermal and superthermal spin-up of grains), the physics and chemistry of molecular formation on grain surfaces (non-spherical grains have larger surface areas for a given grain volume), etc. Some workers have considered fractal grains that are “grown” numerically by sticking simple spherical grains together, while others have considered grains that are shaped like tiny needles or whiskers (e.g., iron whiskers) and solved treated them like classical “antennas” to work out their interaction with light. We expect that true grain shapes are indeed “fractal” in nature, although whether introducing the mathematics of fractals into the problem is actually enlightening remains to be seen.

Grain Sizes

One way to approach the intrinsic size distribution of grains is to consider a model in which grains grow by steady accretion; two smaller grains collide and stick to form a bigger grain, interstellar atoms collide with and stick to grains, so forth.

Consider simple atomic accretion (no grain-grain sticking). This is the treatment originally considered by Oort & van de Hulst in 1946. The time derivative of the grain mass, M_{gr} , is given by

$$\frac{dM_{gr}}{dt} = (N_A v_A) (\pi a^2) \xi m_A$$

Here $(N_A v_A)$ is the flux of atom A, πa^2 is the grain's geometric cross-section, ξ is the “sticking probability”, and m_A is the mass of the atom. The mass of a grain is

$$M_{gr} = \frac{4\pi}{3} \rho_{gr} a^3$$

hence

$$\frac{dM_{gr}}{dt} = 4\pi a^2 \rho_{gr} \frac{da}{dt}$$

And the mean thermal velocity of atom A is

$$v_A = \left(\frac{3kT}{2m_A} \right)^{1/2}$$

Solving for da/dt gives:

$$\frac{da}{dt} = \frac{N_A v_A \pi a^2 \xi m_A}{4\pi \rho_{gr} a^2} = \frac{N_A v_A}{4\rho_{gr}} \xi m_A$$

Unless ξ is a function of size, a , da/dt is independent of a !

For typical ISM conditions, $T \approx 100\text{K}$, $m_A \approx 16$ (Oxygen), and assuming the extreme case of perfect sticking ($\xi = 1$):

$$\frac{da}{dt} = 3 \times 10^{-15} \text{ cm yr}^{-1} \approx 0.3 \mu\text{m} / 10^{10} \text{ yr}$$

Even this over-simplified model lets us build relatively large interstellar dust grains in the ISM within a Hubble time. For more realistic assumptions, it is clearly a problem to form grains by atomic accretion in the ISM. Attempts to add grain-grain sticking collisions do not greatly improve things, because if the collisions are fast enough the grains are more likely to shatter than coalesce.

Observationally it appears that most dust grains are formed in the dense outflowing winds of cool AGB and Red Giant stars, old planetary nebulae, and the cooling envelopes of novae, rather than in the ISM proper. Many outflows from evolved stars are noticeably dusty, and there is an extreme class of very dusty late AGB stars (the OH IR stars) that emit most of their bolometric luminosity at mid- to far-infrared wavelengths due to dust forming in the expanding outer envelopes, even though the stellar photosphere buried within has a much higher temperature that would make it a bright (if red) star at visible wavelengths. These stars are literally dust factories, and calculations suggest that they and others create most of the interstellar dust observed.

Grain formation is offset by grain destruction, the primary mechanisms being a combination of photoerosion by UV light (especially near O and B stars) and destruction in Supernova blast waves. It is clear from current treatments of grain formation and destruction, however, that something is seriously wrong with our models, as they predict that dust is destroyed by SNe shocks more quickly by many orders of magnitude than it is formed in cool stars. People have tried to fall back on formation in the ISM, but the formation timescale appears to be prohibitive.

Grain Mixture Models

However grains form, the canonical treatment assumes (not unreasonably) that the distribution of grain sizes is a power-law, both as a computational convenience and as a prediction of reasonable growth models. Multi-component grain models are also required to explain the observed interstellar extinction curve, as the detailed structure in the extinction curve cannot be due to one type of grain composition with one size distribution.

The first comprehensive interstellar dust models is that of Mathis, Rumpl, and Nordsieck (MRN: 1977, ApJ, 217, 425). They assumed a simple power-law size distribution of the form:

$$N(a) \propto a^{-\beta}$$

with grains ranging in size between some a_{\min} and a_{\max} . The “MRN mixture” is composed of six different grain materials: Graphite (C), Silicon Carbide (SiC), Iron (Fe), Magnetite (Fe_3O_4), Olivines, and Pyroxenes.

Any combination of two materials from this list was gave reasonable fits to the observed interstellar extinction curve between 1100\AA and $1\mu\text{m}$, provided that at least one of the two materials was graphite. MRN concluded that most of the extinction in the galaxy is due to Graphite, with silicates of various kinds mixed in.

There are, of course, problems with the MRN mixture:

- 1) The optical properties of all of the silicate materials under the conditions in interstellar space are fundamentally unknown. In particular, the index of refraction, μ , can be substantially different than laboratory “pure sample” values due to the effects of “damage” by UV photons or cosmic-rays. Similarly, all of these materials have temperature-dependent indices of refraction.
- 2) Nobody knows the appropriate optical properties to use for graphite for interstellar conditions. Graphite has different refractive indices, μ , for its different structure planes, but nobody is sure which plane to assume. And they are temperature dependent.
- 3) The steepness of the power-law for the grain-size distribution makes the fits to the observed interstellar extinction curve insensitive to the lower mass limit (the Rayleigh-Scattering limit) and the maximum size (“gray” scatterers).

Draine & Lee [1984, ApJ, 285, 89, with tables in 1985, ApJS, 57, 587] updated the MRN mixture by introducing improved optical properties, including temperature-dependent indices of refraction, and included fits to extinction measurements at longer wavelengths (at the time of the MRN paper the measurements of the interstellar extinction curve beyond $1\mu\text{m}$ were uncertain). Another innovation was to introduce a fictitious “interstellar silicate”, a component with the imaginary part of the index of refraction contrived to make the visible and IR parts of the extinction curve agree with observations of the extinction towards the Trapezium cluster in the Orion Nebula. In the Draine & Lee mixture, graphite still constitutes most of the interstellar extinction from UV to visible wavelengths, with silicates dominating in the IR from $10\text{--}50\mu\text{m}$, and graphite again becoming dominant for $\lambda \geq 70\mu\text{m}$ into the FIR, but now with $Q_{\text{abs}} \propto \lambda^{-1.5}$. For $\lambda \geq 1\text{ mm}$, observations show that $Q_{\text{abs}} \propto \lambda^{-2}$, but the material responsible is unknown.

All of these previous silicate+graphite models were proposed before the importance of hydrocarbons, particularly PAHs, were fully understood. More recent models, particularly those of Désert et al. [1990, A&A, 273, 215] and Weingartner & Draine [2001, ApJ, 548, 296], have added PAHs to the mix. In these models, carbon is primarily in the form of PAHs when the grains are small, and as the

grains grow they start to behave more like bulk graphite in their optical and material properties. These models also consider grain size distributions that depart, sometimes considerably, from simple power laws, and are arguably more realistic.

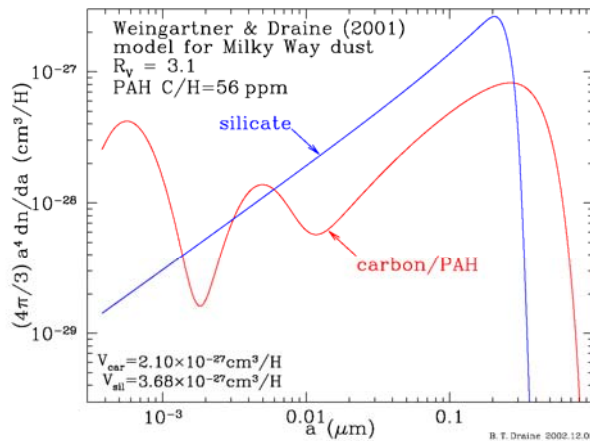


Figure 8: Size distributions for carbonaceous-silicate grain model of Weingartner & Draine (2001a) for Milky Way dust with $R_V = 3.1$, but with abundances decreased by a factor 0.93 (see text).

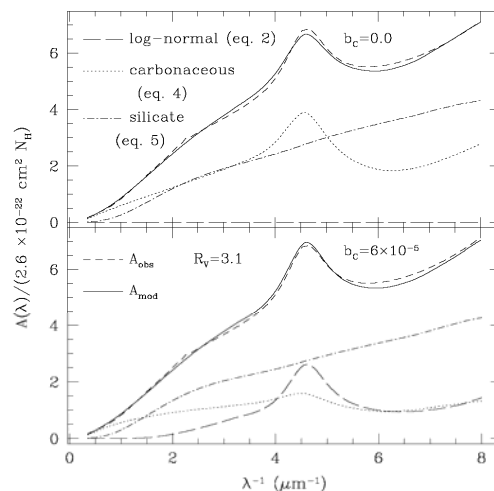


Fig. 11. Dashed line: average diffuse cloud extinction curve. Solid lines: model extinction curve for two extreme values of the ultrasmall carbonaceous grain abundance: $b_C = 0$ (no PAHs) and $b_C = 60\text{ppm C}$ in PAHs. For each case the size distribution of carbonaceous and silicate grains was adjusted to obtain good overall agreement with the observed extinction. From Weingartner & Draine (2001a).

Dust Grain Formation

Observationally, most dust grains are formed in the atmospheres of Red Giant stars and Planetary Nebula envelopes. In these objects we find the ideal conditions for dust formation: high densities ($\sim 10^9 \text{ cm}^{-3}$) coupled with gas kinetic temperatures close to the condensation temperatures of many heavy elements (1000–2000K). However, once formed, the grains can be broken into smaller units by a combination of sputtering and grain-grain collisions, or grow by coagulation or by the accretion of atoms and molecules onto their surfaces (adsorption). Novae are also observed sites of dust formation, and while Supernovae have been implicated direct evidence of dust formation in SNe is still lacking except in all but a few specific (and arguable) cases.

Stellar envelopes in the late stages of stellar evolution (the AGB and planetary nebula envelope ejection phases) appear to be the primary breeding ground for solid particles that become interstellar dust grains. The source stars are divided into two basic classes by their relative O/C abundances:

O>C (Oxygen Rich):

The atmosphere of the Sun and the diffuse ISM are Oxygen rich by this definition. The principal condensates are silicates as most of the C is locked up as CO. Observations show that the dusty outflows from O-rich stars have very strong 10 μ m silicate features in their spectra.

O<C (Carbon Rich):

This occurs in Carbon Stars where nucleosynthesis and dredge-up have raised the atmospheric C abundances very high. The principal condensates are carbonaceous solids like graphite and amorphous carbon. The 10 μ m silicate feature is notably absent in the mid-IR spectra of carbon stars, but some show a weak 11.3 μ m SiC emission feature. Some carbon-rich post-AGB stars also show a feature at 20.1 μ m that has been tentatively identified with TiC grains (called TiC clusters or “nanocrystals” by material scientists).

After injection of dust grains into the ISM from stellar mass-loss in the late phases of evolution (post-AGB envelope ejection), additional processes contribute to grain growth and destruction:

- 1) Accretion of atoms, ions, and molecules onto grain surfaces (as described earlier)
- 2) Grain-Grain collisions in dense clouds. This results in coagulation (formation of larger grains), rebound (heating but no growth), and shattering and evaporation (destruction of grains).
- 3) Photodesorption of atoms and molecules from grain surfaces.
- 4) Photolysis of ice mantles and other surface coatings by UV starlight.
- 5) Destruction by Supernova blast waves.

As mentioned before, attempts to model the growth and destruction equilibrium in order to derive the typical grain size distribution are currently in crisis, as they predict that grains should be wiped out by SNe far faster than they are made in stellar envelopes. This is tantamount to our current state of knowledge of dust formation/destruction being that the models say dust shouldn't exist in the ISM! This is a topic at the ragged edge of research on interstellar dust. At present, there are no reliable a priori models of the formation and destruction of interstellar dust grains.

IV-4 Interstellar Polarization

In addition to absorbing and scattering light passing through the ISM, aligned elongated dust grains can polarize the light. The polarization of starlight by the ISM was first observed by Hiltner & Hall in the 1940s [Hiltner 1949, ApJ, 109, 471; Hall 1949, Science, 109, 166]. This observation clearly demonstrated that dust grains were non-spherical, and that they had to be globally aligned, presumably by large-scale magnetic fields.

Polarization due to interstellar dust is a result of “linear dichroism” in non-spherical grains. Recall that the extinction efficiency of a grain, Q_{ext} , depends on the grain’s cross-section. This means that the effective Q_{ext} along the long-axis of an elongated grain is greater than that along the shorter (perpendicular) axis. Light waves with electric vectors aligned with the long-axis of a grain will see a higher effective Q_{ext} and experience greater extinction than waves with their electric vectors perpendicular to the long axis of the grain. This means that if purely unpolarized light enters a region with aligned dust grains, those waves with electric vectors perpendicular to the grains will suffer from less extinction, and emerged polarized. For the case of idealized, spinning cylindrical dust grains, the resulting polarization is proportional to the difference in the minimum and maximum extinction efficiencies:

$$P = \frac{1}{2} n_{gr} \sigma_{gr} (Q_{\text{ext}}^{\text{max}} - Q_{\text{ext}}^{\text{min}})$$

We therefore expect to observe a correlation between the polarization along a given line of sight, P , and the amount of selective extinction, A_{λ} , such that

$$\frac{P}{A_{\lambda}} = 0.46 \frac{Q_{\text{ext}}^{\text{max}} - Q_{\text{ext}}^{\text{min}}}{\bar{Q}_{\text{ext}}}$$

Here \bar{Q}_{ext} is the mean extinction efficiency for the grain, which is a function of λ .

In general, unreddened stars are unpolarized. For reddened stars, the observed polarization at visible wavelengths is seen to range from unpolarized up to a maximum value given approximately by:

$$P_{\text{max}} \leq 0.03 A_{\lambda_{\text{max}}} \text{ mag}^{-1}$$

Where $A_{\lambda_{\text{max}}}$ is the extinction at λ_{max} . In stars polarized by interstellar dust, the wavelength dependence is observed to obey an empirical relation known as the “*Serkowski Law*”:

$$P_{\lambda} = P(\lambda_{\text{max}}) e^{-K(\ln(\lambda/\lambda_{\text{max}}))^2}$$

The Serkowski Law depends on two parameters, λ_{max} and K :

λ_{max} is the wavelength of the maximum observed polarization. K was originally found to 1.15 and considered a constant, but recent work (e.g., Wilking et al. 1982) has found that K in fact depends on λ_{max} like

$$K \approx 1.02(\lambda_{\text{max}} / 5500) - 0.10$$

where λ_{max} is in \AA . The observed features of the Serkowski Law are as follows:

1. λ_{max} has a mean value of $\sim 5500 \text{\AA}$, but ranges between 3400\AA and up to $1 \mu\text{m}$.
2. The polarization, P_{λ} , rises from the UV to a peak in the visible, then falls through the visible to the NIR. This is different than the monotonic decrease in extinction, A_{λ} , from the UV to

NIR. This suggests that the grains responsible for UV extinction do not contribute to the polarization (supporting the general idea that there is a mix of grains).

3. The observed value of λ_{\max} also seems to be roughly proportional to R_V , but with significant scatter compared to the scatter in R_V determined by measuring the extinction law. For λ in \AA , this is approximately:

$$R_V \approx \frac{5.5\lambda_{\max}}{10000}$$

4. In the NIR ($0.9 \leq \lambda \leq 5\mu\text{m}$), the polarization has a power-law form like

$$P_\lambda \propto \lambda^{-1.8}$$

For most regions, the power-law index varies between 1.5 and 2, but is similar to the approximate power-law form of the extinction in this same region:

$$A_\lambda \propto \lambda^{-1.7-1.8}$$

Note that this is the *absolute* P_λ , not polarization measured relative to the maximum polarization, $P(\lambda_{\max})$. The observed NIR P_λ relation is apparently independent of R_V (unlike the case for visible-wavelength polarization).

This independence suggests that the size distribution of large grains (responsible for NIR extinction) is roughly the same in the diffuse ISM (where $R_V \approx 3$) and in dense clouds (where $R_V \approx 5$).

The maximum value of the ratio of the $P(\lambda_{\max})$ to the extinction at λ_{\max} is 0.03 mag^{-1} , much less than the value of 0.22 mag^{-1} expected from ideal cylindrical grains. This raises the following questions:

1. Are there separate types of grains, only some of which are aligned?
2. Are all grains aligned, but with some having shapes that are sufficiently different from ideal cylinders to make them inefficient polarizers?
3. Is there always some randomly oriented magnetic field component that de-aligns some fraction of the grains (de-alignment here in an ensemble sense rather than at the level of individual dust grains)?

Grain Alignment

Off-center collisions of grains with atoms and molecules will impart rotational as well as translational kinetic energy. In the absence of non-conservative torques, elastic collisions will result in the following relationship between the rotational energy imparted by collisions and the temperature of the colliders:

$$\frac{1}{2} I \langle \omega_r^2 \rangle = \frac{1}{2} kT$$

Here T is the kinetic temperature of the gas and I is the moment of inertia of the grain. For simple spherical grains with mass M and radius a ,

$$I = \frac{2}{5} Ma^2$$

For typical assumed grain densities of $\rho_{\text{gr}} \approx 1 \text{ g/cm}^3$ and interstellar gas temperatures of 100K, this lets us compute the RMS rotation rate:

$$\langle \omega_T^2 \rangle^{1/2} = \left(\frac{kT}{I} \right)^{1/2} = \left(\frac{15}{8\pi} \frac{kT}{\rho_{gr} a^5} \right)^{1/2}$$

This yields thermal rotation rates of:

$$\begin{aligned} \langle \omega_T^2 \rangle^{1/2} &= 1.8 \times 10^5 \text{ s}^{-1} & a &= 0.3 \text{ } \mu\text{m} \\ \langle \omega_T^2 \rangle^{1/2} &= 2.9 \times 10^5 \text{ s}^{-1} & a &= 0.01 \text{ } \mu\text{m} \end{aligned}$$

Thus we expect that interstellar grains should be rapidly rotating just from “thermal spin-up” alone. For non-spherical grains, the moment of inertia, I , differs along each of the principal axes. In general, one replaces the grain radius, a , by an effective radius, a_{eff} , and modifies the spherical grain moment of inertia by a factor α_j , where the subscript j refers to the specific body axis under consideration. For rotation about the principal axis, $j=1$, we have:

$$\omega_T^2 = \frac{15}{8\pi\alpha_1} \frac{kT}{\rho_{gr} a_{\text{eff}}^5}$$

Since α_1 is of order 1 even for complex grain shapes, the thermal rotation rates are roughly comparable for spherical and non-spherical grains.

The presence of a magnetic field will introduce small non-conservative torques that cause grains to align their spin-axes (statistically) with the magnetic field. One mechanism for explaining magnetic alignment of grains is Paramagnetic Relaxation, also called Paramagnetic Dissipation or the “Davis-Greenstein Mechanism” (after Davis & Greenstein 1957, ApJ, 114, 206). When a paramagnetic material is drawn through a magnetic field, the imaginary part of the magnetic susceptibility determines the amount of energy absorbed due to the changing magnetization of the material. The absorption of energy results in a torque that causes the grains to relax into rotation about their short axes with this axis aligned with the magnetic field. This results in the long axes of the grains becoming oriented perpendicular to the magnetic field lines on average.

If the spins of the grains are driven entirely by random thermal collisions, and they are torqued by weak magnetic fields through paramagnetic dissipation, the grains will align on the Davis-Greenstein timescale:

$$\tau_{DG} \approx 1.6 \times 10^{11} \frac{a_{\text{eff}}^2 \rho_{gr} T_{gr}}{B^2} \text{ seconds}$$

Here T_{gr} is the internal temperature of the dust grain, and enters through the temperature-dependence of the magnetic susceptibility of the grain. For typical grain parameters, this relation predicts relaxation times of between 10^7 and 10^{12} years.

There are two problems with the Davis-Greenstein mechanism:

1. The magnetic fields required for reasonable relaxation times ($\sim 10^7$ years) are of order 10-100 μG . This is much larger than the observed field strengths of $\sim 1 \mu\text{G}$.
2. The relaxation time scales like a^2 , predicting *greater* alignment among smaller grains than larger grains. This is exactly the opposite of what is observed (the Serkowski law suggests that the smaller grains responsible for UV extinction do not contribute significantly to the polarization).

Two classes of solutions have been proposed:

Superparamagnetic Grains:

This proposes that grains can have small metallic inclusions of magnetite or other magnetic materials that enhances the coupling with the magnetic field, decreasing the alignment time. At least one such inclusion is required in big grains, but small grains would not have enough room for these inclusions, and so it would be statistically unlikely for small grains to have inclusions. This is generally consistent with the empirical result that large grains are primarily responsible for polarization as deduced from the Serkowski law.

Superthermal Rotation:

Consider a grain embedded in a hot gas. Since there is no preferred direction for the colliding gas particles to come from, thermal rotation builds up slowly. However, if this symmetry can be broken, the result would be a systematic torque that can rapidly spin-up the grain well beyond the thermal rotation rate (hence “superthermal rotation”).

A superthermal rotation mechanism proposed by Purcell [1979, ApJ, 231, 404] uses molecular hydrogen (H_2) formation on grain surfaces to provide the kicks. H_2 molecular formation on grains occurs at specific sites on the grain surface that are not necessarily distributed isotropically. The systematic torque due to H_2 formation can quickly spin up the grain to 10–100 \times the thermal rotation rate. Other contributing effects include variations in the stickiness of the grain surface to atomic and molecular collisions, the efficiency of photoelectron emissivity (the photo-ejected electron gives the grain a kick), etc.

Draine & Weingartner [1996 ApJ, 470, 551 & 1997 ApJ, 480, 633] have shown that radiative torques due to the interstellar radiation field can also induce superthermal spin-up. In diffuse interstellar clouds, they find that radiative torques can drive large grains ($a_{\text{eff}} \geq 0.1 \mu\text{m}$) to extreme superthermal rotation ($\omega_{\text{rad}} > 300\omega_T$), and will dominate over H_2 formation torques. For small grains ($a_{\text{eff}} \leq 0.05 \mu\text{m}$), H_2 formation torques will dominate, but due to the randomizing effect of variations in the formation rate across the grain surface, the spin-up is less (few times ω_T) and smaller grains will be less aligned. The spin-up rate is enough to be consistent with alignment due to the Davis-Greenstein mechanism. However, if the local radiation field is more than 1% anisotropic, torques due to this anisotropic component can rapidly spin-up the grains, and lead to alignment of the grains with the magnetic field more efficiently than the Davis-Greenstein mechanism. Further, even if H_2 formation-torques dominate spin-up, radiation torques due to anisotropic starlight will dominate alignment.

In summary, the understanding of the causes of grain alignment is currently undergoing substantial revision over the old Davis-Greenstein mechanism. It does not yet appear that we can distinguish between the competing ideas suggested to explain grain alignment. The literature is also complex, and it depends upon how one treats the detailed shapes and compositions of the grains, neither of which are well understood at present.

Other Manifestations of Dust Polarization

In addition to “transmission polarization” due to linear dichroism in a population of aligned dust grains, there are two other manifestations of dust polarization: scattering polarization and Far-IR emission polarization.

Scattering polarization:

Scattering polarization occurs in reflection nebulae and embedded sources. Single scattering of starlight off of a nearby cloud induces polarization perpendicular to the projected line-of-sight between the source and the scattering cloud. The top and face-on views of the scattering polarization geometry are illustrated in Figure IV-3.

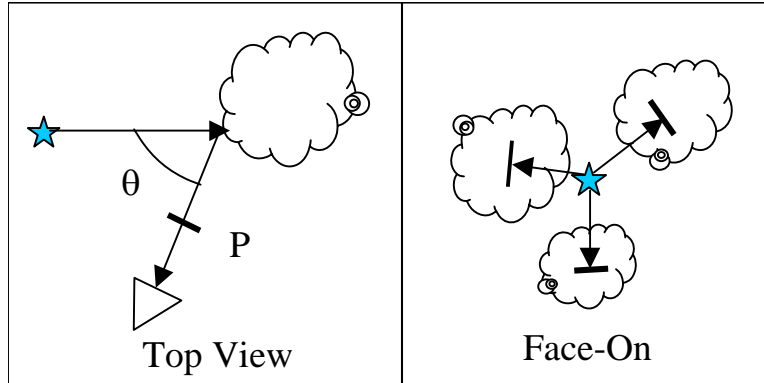


Figure IV-3: Schematic of single-scattering reflection polarization.

The wavelength dependence enters from the wavelength-dependence of the grain albedo (ratio of the scattering to extinction efficiencies). It is complicated, however, by the fact that the scattering is anisotropic and strongly forward scattering. The scattering anisotropy is quantified in terms of an anisotropy parameter, g :

$$g \equiv \langle \cos \theta \rangle$$

Here θ is the scattering angle (see Figure IV-3). Isotropic scattering has $g=0$. At visible and near-IR wavelengths, the anisotropy factor is estimated to be ~ 0.7 , but the derivation from the observations depends strongly on you choice of grains, especially in the ultraviolet. Multiple scattering is also possible, but is a terrible mess beyond the scope of these notes.

Far-IR Emission Polarization:

Aligned grains located deep inside molecular clouds (e.g., the Orion Complex or M17) can produce polarized emission. Large grains heated to equilibrium temperatures of 30–50K radiate primarily at wavelengths of 60–100 μm . Because the emission efficiency is greater along the long axis of the grains than along the short axis, there is a net polarization of the thermal emission aligned parallel to the long axis (compare this to transmission polarization that is always *perpendicular* to the long-axis).

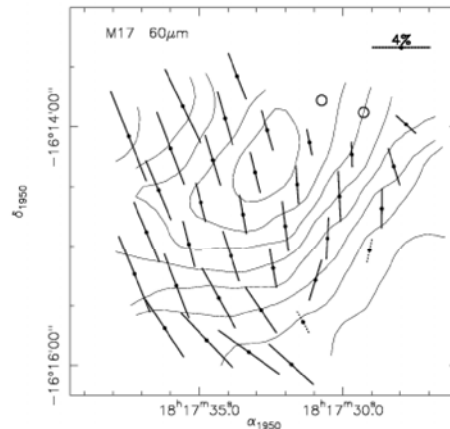


Fig. 37. 60 μm linear polarization toward M17. Flux contours are at 20%, 30%, ...,90% of the peak flux. From Dotson et al (2000).

Examples of Far-IR emission polarization, observed with the Kuiper Airborne Observatory may be found in Hildebrand, Dragovan, & Novak [1984, ApJL, 284, L51], and Dragovan [1986, ApJ, 308, 270] for the Orion OMC1 complex, Werner et al. [1988, ApJ, 333, 729] for the Galactic center (molecular torus), and Dotson [1996, ApJ, 470, 566] for M17 to name a few.

IV-5 Emission by Dust Grains

Up to now we have primarily considered how grains interact with light passing through them, but now we will consider grains as sources of light. Kirchoff's Law tells us that bodies that are good absorbers must also be equally good radiators. The rise of IR, Far-IR, and sub-millimeter wavelength astronomy has given us a great deal of insight into the nature of thermal emission from dust grains. In general, the equilibrium temperatures of grains are in the range of 30–50K or more, which means they radiate predominantly at far-IR wavelengths of 50–100 μ m. Note that grains are not blackbodies, but radiate instead as modified blackbodies with a strongly wavelength-dependent emissivity, as we shall see.

While most grains are nearly perfect scatterers in terms of their optical properties (i.e., $Q_{\text{scat}} \gg Q_{\text{abs}}$), it must be emphasized that Q_{abs} , however small, is non-zero. As such, some of the incident photons are absorbed by the grain and cause it to heat up. As we saw, grains preferentially absorb/scatter bluer (and hence more energetic) photons, so the amount of heating per photon is considerable. The hot grain re-radiates this energy as thermal continuum radiation at far-IR wavelengths.

Dust grains are not blackbodies. In general, grains are very inefficient radiators at long wavelengths, with an emission efficiency of $Q_{\text{em}} \propto \lambda^{-1} - \lambda^{-2}$. This means that grains will have an equilibrium temperature that is *hotter* than the temperature of a perfect blackbody immersed in the same radiation field.

Grain Heating and Cooling

There are a number of ways that a dust grain may be heated:

1. Absorb a photon of starlight
2. Collisions with atoms, electrons, cosmic rays, or other dust grains
3. Absorb energy from chemical reactions occurring on grain surfaces (e.g., H₂ formation)

Radiative heating of dust grains is expected to be important because of the large energy density of starlight ($\sim 0.5 \text{ eV cm}^{-3}$) and the grain's high opacity to starlight.

A grain struck by a photon can leave that grain in an excited state, with a probability of $\sim 10^7 \text{ s}^{-1}$ for spontaneous re-emission. Complex molecules making up grains have many excited states, and can quickly (10^{-12} sec) redistribute that energy into internal vibrational states, heating the grain. Since the product of the spontaneous emission probability and vibrational redistribution timescale is $\sim 10^{-5}$, we expect that most photon absorptions will efficiently heat the grain.

Once heated, grains can cool via a number of channels:

1. Emit a thermal photon
2. Collide with cold atoms or molecules
3. Ejection (sublimation) of atoms or molecules from the surface of the grain

Under most ISM conditions, radiative cooling is expected to dominate and setup equilibrium.

Equilibrium heating of grains

Consider a spherical dust grain with radius a located a distance d away from a star with luminosity $L_{\nu}(\ast)$. The balance between energy absorbed by the grain and thermal energy emitted by the grain is given by:

$$\pi a^2 \int_0^{\infty} \frac{L_{\nu}}{4\pi d^2} Q_{\text{abs}}(\nu) d\nu = 4\pi a^2 \int_0^{\infty} Q_{\text{em}}(\nu) \pi B_{\nu}(T_{\text{gr}}) d\nu$$

The left side is an integral over the product of the incident flux per unit frequency from the star at distance d and the effective absorption cross-section of the grain (the geometric cross-section of the grain multiplied by $Q_{\text{abs}}(\nu)$, the absorption efficiency). On the right-hand side is the surface area of the grain, multiplied by the emitted spectrum, which is a blackbody with temperature T_{gr} modified by an emission efficiency $Q_{\text{em}}(\nu)$.

The star emits primarily at UV, visible, and near-IR wavelengths, where as we have seen before the absorption efficiency scales as roughly ν^{1-2} , so most of the grain absorption is also preferentially in the UV/visible/near-IR range. Most of the emission, however, is in the mid- to far-IR, because of the small dust temperature (typically a few 10s of Kelvin to at most a couple of hundred K).

For the purposes of making order-of-magnitude estimates, it is conventional to evaluate the integrals by recognizing that the grain size distribution cancels out to first order, and then introducing two averaged quantities to replace the absorption and emission efficiencies:

$$\langle Q_{\text{UV}} \rangle = \text{Planck-averaged absorption efficiency in the UV.}$$

$$\langle Q_{\text{IR}} \rangle = \text{Planck-averaged emission efficiency in the IR.}$$

Thus, to within an order of magnitude, the equation of thermal balance becomes:

$$\frac{L_*}{4\pi d^2} \langle Q_{\text{UV}} \rangle \approx 4 \langle Q_{\text{IR}} \rangle \sigma T_{\text{gr}}^4$$

Here L_* is the total luminosity of the star located distance d away, and σ is the Stefan-Boltzmann constant. Solving for the dust temperature gives:

$$T_{\text{gr}} \approx \left(\frac{\langle Q_{\text{UV}} \rangle}{\langle Q_{\text{IR}} \rangle} \right)^{1/4} \left(\frac{L_*}{16\pi\sigma d^2} \right)^{1/4}$$

Note that as expected the temperature of the grain gets cooler the further it gets from the star.

In general, $\langle Q_{\text{IR}} \rangle$ is a function of both T_{gr} and the grain size, a . Simple expressions can be derived to give us some feeling for the behavior of the grain temperature by assuming that the grain emissivity scales like $Q_{\nu} \propto \nu^p$, where $0 < p < 2$.

$$\text{For } Q_{\nu} \propto \nu^1, \langle Q_{\text{IR}} \rangle \approx 2 \times 10^{-3} a_{\mu\text{m}} T_{\text{gr}}$$

$$\text{For } Q_{\nu} \propto \nu^2, \langle Q_{\text{IR}} \rangle \approx 4 \times 10^{-6} a_{\mu\text{m}}^2 T_{\text{gr}}^2$$

Where a is the grain size in microns (see Draine et al. 1980, ApJ, 238, 140). The total IR flux from the grain, $\langle Q_{\text{IR}} \rangle \pi B_{\nu}(T_{\text{gr}})$, therefore scales like T_{gr}^5 or T_{gr}^6 depending on the slope of the emissivity law. This is much steeper than the T_{gr}^4 scaling expected for a perfect blackbody.

It must be borne in mind that Q_{ν} depends critically on the compositions and sizes of the grains in question. For example, for amorphous carbon grains (e.g., Draine 1981, ApJ, 245, 880):

$$\langle Q_{\text{IR}} \rangle = 6.7 \times 10^{-4} a_{\mu\text{m}} T_{\text{gr}}$$

Again with a in microns. Other grains have different emissivities (see, for examples, the figures in Draine & Lee 1984, cited in the section on dust mixtures).

The dust “temperature” derived from the observed spectrum will thus depend critically on the form of assumed emissivity law. For example, as the power law index of Q steepens (e.g., Q_{λ} changes from

λ^{-1} to λ^{-2}), the grains become inefficient radiators at long wavelengths, shifting the peak of the emergent spectrum towards shorter wavelengths. The result is a spectrum that *looks* hotter than a typical blackbody (e.g., as per Wien's Law).

The infrared cirrus detected at Far-IR wavelengths by IRAS and COBE/DIRBE is from dust grains in thermal equilibrium with the interstellar radiation field. This gives it a more or less uniform temperature across the sky of 18–21K. Emission from the Cirrus dominates the appearance of the ISM at wavelengths of 100 μ m and longer. Dust grains heated by individual stars or star clusters in dusty environments (e.g., reflection nebulae or star formation regions) have somewhat higher equilibrium temperatures, in the 40–80K range, with emission peaking near 60 μ m.

Thermal emission from equilibrium-heated dust grains dominates the Far-IR continuum emission from galaxies, contributing as much as 30–50% of the bolometric luminosity of the Milky Way. This means in effect that about half of the starlight emitted in the Galaxy is absorbed and re-radiated by dust. In other galaxies, the Far-IR continuum ranges widely: from <1% of the total bolometric luminosity in E and S0 galaxies with little or no interstellar dust and gas, to nearly 100% in the most extreme starburst galaxies (so-called Ultraluminous Far-Infrared Galaxies or ULIRGs).

Dust Masses

A quantity often derived from the observed thermal dust spectrum is an estimate of the total mass of dust present in a region (e.g., the dust mass integrated over a galaxy observed in the Far-IR with IRAS or ISO).

The observed spectrum of optically thin dust will be a modified blackbody spectrum:

$$L_\nu = N_{gr} 4\pi a^2 Q_\nu(a) \pi B_\nu(T_{gr})$$

Where N_{gr} is the total number of dust grains in the galaxy, and a is a typical size (assuming spherical grains). The usual dust emissivity law is:

$$Q_\nu \approx \left(\frac{2\pi a \nu}{c} \right)^\beta$$

As before, the power-law index, β , has values between 1 and 2. The total mass is related to the number of grains and their individual masses. For spherical grains of a given characteristic size (usually taken to be $a=0.1\mu$ m), and a typical mean grain density of $\rho_{gr}=2 \text{ g cm}^{-3}$:

$$M_{gr} \approx N_{gr} \frac{4\pi}{3} a^3 \rho_{gr}$$

The usual practice is to compute the flux ratio at two wavelengths, e.g. 60 and 100 μ m, as the flux ratio is independent of the distance to the source (observed flux scales like $1/d^2$), and from this estimate T_{gr} given an assumed emissivity power-law index. Given T_{gr} one can then derive the dust mass given an estimate of the distance to the source.

The primary source of systematic uncertainty in estimating M_g comes from not knowing a priori the power-law index of the emissivity. In the literature, estimates of the dust masses of galaxies are often based on 60 μ m/100 μ m flux ratios derived from IRAS observations where this problem is especially acute. While one can estimate the dust temperature to within about 10K with 60/100 μ m fluxes despite choice of the assumed slope of the emissivity, the resulting dust mass estimates can differ by over 2–3 orders of magnitude. The best estimates of the temperatures and masses of dust are derived from observations at millimeter and submillimeter wavelengths (e.g., 450 μ m, 800 μ m and 1mm

windows now being opened by advances in submillimeter detector technology like the SCUBA array at the JCMT). These bands are in the long-wavelength limit for $0.1\mu\text{m}$ dust grains, where the emissivity law is expected to have a power-law index of very nearly 2.

Non-Equilibrium Heating of Tiny Grains

When dust grains become physically very small, to the point that they are composed of fewer than 100 individual atoms, the amount of heating induced by the absorption of ambient UV photons becomes strongly time-dependent. Time-dependent heating cannot be treated as an equilibrium process, as was the case with large grains, and we must consider the impact of *single* UV photons on the grain instead of integrating over the incident spectrum in a time-independent manner.

The amount of energy E needed to heat an object (solid, gas, or liquid) by an amount ΔT is given by

$$E = C_V \Delta T$$

C_V is the heat capacity of the object. In the high-temperature limit the heat capacity of an object composed of N atoms is:

$$C_V = 3Nk$$

$3N$ is the number of thermodynamic degrees of freedom in the object (e.g., internal vibrational degrees of freedom in a solid particle), and k is Boltzmann's constant. The relative temperature increase, ΔT , is related to the photon energy, $h\nu$, by:

$$\Delta T \approx \frac{h\nu}{3Nk}$$

Large grains will only heat up a small amount in response to absorbing a single-photon. If a grain is sufficiently small, the energy of a *single* UV photon will be larger than the grain's internal heat capacity, and the resulting instantaneous heating ΔT will be very large: a tiny grain with only 30 internal degrees of freedom that absorbs a 10eV UV photon will heat up by $\Delta T \approx 1000\text{K}$.

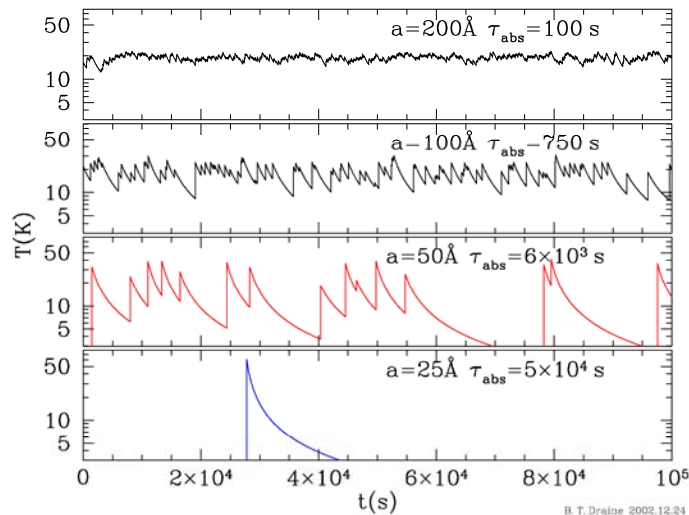


Figure 13: A day in the life of 4 carbonaceous grains, heated by the local interstellar radiation field. τ_{abs} is the mean time between photon absorptions (Draine & Li 2001).

The smaller the grain, the faster the cooling time, so a tiny grain will spend very little time in a high-temperature state before radiatively cooling. The temperature of the grain will therefore be strongly time-dependent, characterized by sharp upward “spikes” in temperature upon absorption of a UV photon, followed by emission of continuum radiation as the object rapidly cools. The tiny grain never achieves equilibrium with the radiation field, and so we say that the grain is “stochastically” heated.

Because the temperature of each grain is time-dependent, an ensemble of tiny grains will have a spectrum that is broader than that of large grains in equilibrium at that same temperature. Another way of saying this is that an ensemble of tiny grains will exhibit a wider range of grain temperatures than equilibrium-heated large grains.

The emergent thermal radiation from an ensemble of stochastically heated tiny grains will be hotter than the radiation emerging from large-scale grains in equilibrium with the *same* radiation field. Large grains will have temperatures of 30–50K and radiate primarily at far-IR wavelengths (50–100 μ m). Tiny grains, by contrast, can have instantaneous grain temperatures of 500–1000K or more, radiating primarily at 1–10 μ m. Kris Sellgren and her collaborators discovered this emission as excess diffuse 1–4 μ m continuum emission in reflection nebulae. As much as 1% of the stellar luminosity is re-radiated by tiny grains in this region, compared to 30–50% emitted by cooler grains in the Far-IR region (50–100 μ m).

Unlike the case of large grains near a star that get cooler as they get further from the star, the temperature of stochastically heated grains is independent of distance. It was this property of stochastically heated grains that was essential to identifying their presence in reflection nebulae as the source of the excess near-IR continuum emission.

In addition to excess continuum in reflection nebulae, tiny grains have invoked to explain a number of otherwise unexplained properties of dusty regions:

- 1) 12 μ m excess emission in the Galaxy ISM detected by IRAS as part of the Far-IR cirrus component (most of which is seen at 100 μ m and has Far-IR “colors” consistent with large grains with $T_{gr} \approx 15$ –20K).
- 2) Emission features at 12 μ m from optically-thin tiny grains, in which some (or all?) of the diffuse 12 μ m emission is due to line emission excited in stochastically heated grains instead of continuum emission.

Two schools of thought have emerged as to the nature of the tiny grains. One view is that they are tiny particles that may be treated semi-classically, as we have done above. The second view notes that a grain with 30–50 atoms is about the same size as very large molecules (e.g., PAHs or more exotic macromolecules like Fullerenes), and so they can be treated quantum mechanically. Both views have something to offer, and the choice is not as black and white as it may appear. One particular area of current research is to understand the connection between tiny grains/large molecules and the unidentified IR bands (i.e., are the tiny grains the “carriers” of the UIR bands). Kris and her collaborators (and competitors) are actively working on this problem.

Dipole radio emission from spinning grains

A spinning charged dust grain emits electric- and magnetic-dipole radiation. As we saw in section IV-4, dust grains are expected to be very rapidly spinning ($\omega \approx 10^{5-7} \text{ s}^{-1}$) due to a combination of thermal and superthermal processes. The grains can also become charged when UV photons from the interstellar radiation field eject electrons from their surfaces. Because the spin axes are expected to be uncorrelated with the axis of the dipole electric field of the charged grain, the component of the dipole moment perpendicular to the spin axis will emit dipole radiation with characteristic frequencies of 10–100GHz (microwaves). Similarly, if the grains are intrinsically magnetized (e.g., grains with a high iron content would be intrinsically ferromagnetic), they might also emit *magnetic* dipole radiation in the same region.

Emission of dipole radiation will result in damping of the grain rotation. For the very smallest grains ($N < 150$ atoms), the emission of dipole radiation can dominate rotational damping, thus limiting their maximum spin rates. For larger grains the rotational damping is dominated by long-range interactions with ions and electrons (“plasma drag”). The net result is a physical mechanism that can set up a distribution of spin rates that depends critically on grain size. Since spin rate is coupled to relaxation timescales for grain alignment with global magnetic fields, this will influence the subsequent polarization properties of the ensemble of grains.

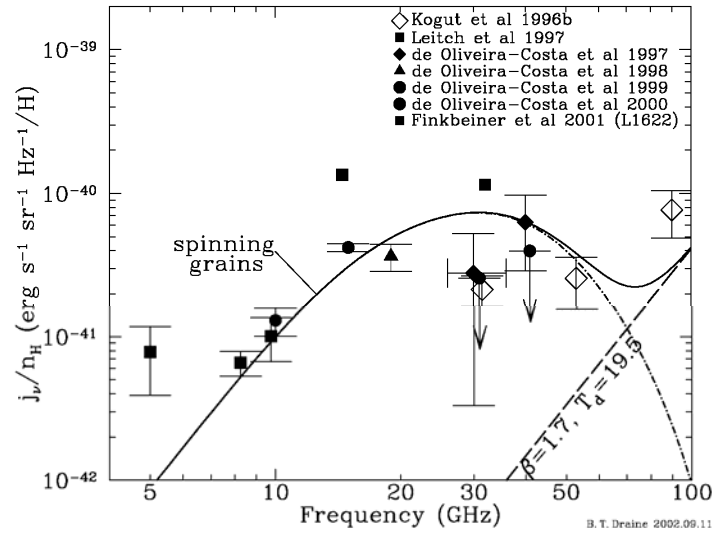


Fig. 16. Microwave sky brightness correlated with $100\mu\text{m}$ emission. Shown is the estimated microwave emissivity per unit H nucleon.

Observationally, dipole emission from spinning small grains has been proposed as the origin of the “anomalous” 14–90GHz microwave background component detected from studies of the Cosmic Background Radiation (Kogut et al. 1996 ApJ, 460, 1; deOliveira-Costa et al. 1997, ApJL, 482, L17; Leitch et al. 1997 ApJL, 486, L23). This radiation was detected as a foreground component correlated with galactic $100\mu\text{m}$ thermal emission from the “infrared cirrus”. This immediately suggested that it is associated somehow with dust grains. The basic theoretical work connecting the two is by Draine & Lazarian [1998 ApJL, 494, L19; 1998 ApJ, 508, 157; and 1999 ApJ, 512, 740]. The agreement between the predictions of the spinning electric dipole grains and the observed anomalous microwave background is quite remarkable.

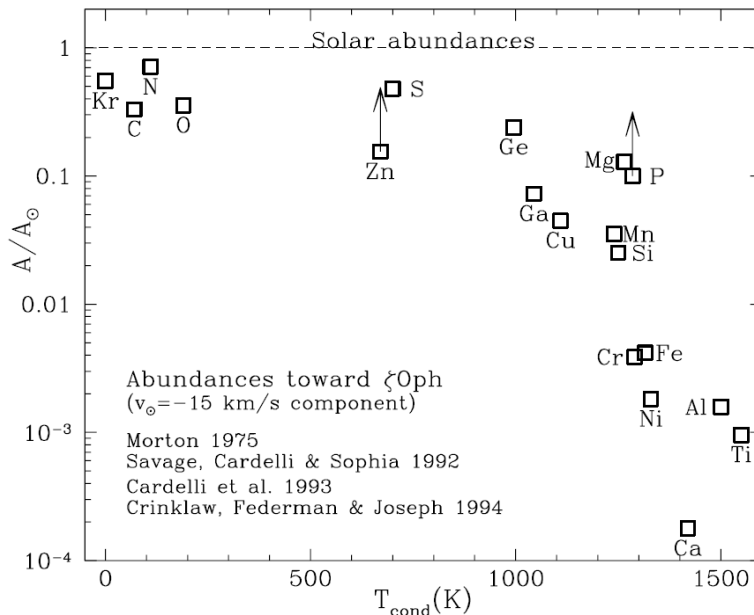
IV-6 Depletion of Elements onto Interstellar Grains

As discussed in the chapter on Neutral Atomic Gas, we can estimate the gas-phase abundances of the diffuse ISM by measuring the relative strengths of interstellar UV and visible-wavelength absorption lines along the line of sight towards bright stars. The observed abundances of many of the heavy elements are strongly depleted relative to solar values, and by inference we conclude that the “missing” atoms are locked up in the solid-phase in dust grains. This removes them from the gas-phase, making them inaccessible to absorption-line studies. The current state-of-the-art of depletion studies was use data provided by the Hubble GHRs, and are described in a classic review article by Savage & Sembach [1996, ARAA, 34, 279].

Observed depletion patterns

In general, the amount of depletion observed appears to depend on the mean Hydrogen number density along the line of sight. Greater depletion is observed in regions of higher density. Cold diffuse clouds also show greater overall depletion than warm diffuse clouds, and there is less depletion along sight lines that pass through the Galactic halo (observed towards bright QSOs).

The strongest correlation is between the amount of depletion and the condensation temperature of the element being depleted. In general, the higher the condensation temperature of an element, the more it will be removed (depleted) from the gas phase. The figure on the following page shows a plot of the depletion of elements relative to solar as a function of the condensation temperature, T_C . As dust grains form in a cooling, expanding AGB star atmosphere, those elements with a high T_C condense out first, and will continue to be depleted further as the atmosphere cools. Elements with lower T_C condense out later, and thus are less depleted by the time that grain formation halts (e.g., when the circumstellar envelope finally dissipates) as they have had less time to get locked into grains.



Pattern of the depletion of gas-phase elements onto dust grains measured towards ζ Oph [from Draine 2003, Saas-Fee Lectures]

The detailed depletion patterns are as follows. In cool clouds

- C, N, O, S, Ar, & Kr and heavy elements like Se, Tl, Sn, and Cl show depletion factors of less than 3, or measurement uncertainties consistent with no depletion.
- P, Zn, and Ge have slightly higher depletion factors, but can be depleted by up to a factor of 10 in regions with $\langle n_H \rangle$ larger than 10 cm^{-3} .
- Ca, Ti, V, Cr, Fe, Co, & Ni all have depletion factors in excess of 100, with Ti and Ca being as much as 1000x less abundant in the gas-phase than the solar abundances.

In the diffuse ISM, the basic patterns of abundances are as follows:

- Fe, Cr, and Si are all 10–100 times depleted, scaling roughly as $\langle n_H \rangle^{1/2}$
- Ca, Ti, & Al show similar depletions to Fe at low $\langle n_H \rangle$, but the depletion factors rise more steeply, roughly as $\langle n_H \rangle$, in denser regions.
- Some elements, notably S, As, Mg, & Cl are virtually undepleted in diffuse clouds, but can be depleted by factors of up to 10 in dense clouds.
- At a given $\langle n_H \rangle$, patterns of depletion show less than 0.3dex of dispersion along different lines of sight. The exception is along sight lines with very strong variations in $\langle n_H \rangle$.

The observed depletion patterns seen in the interstellar medium are therefore giving us important information on the formation and destruction histories of the grains. What elements will be depleted depends on the environment of the grains during formation (i.e., grains forming in regions with very different abundances will result in different depletion patterns). Similarly, as destroyed, they return elements to the gas phase, altering the depletion pattern. The research challenge is how to translate the depletion pattern into the grain history.

One important lesson to be imparted here is that in dusty regions, the gas-phase abundances derived from observations of either absorption or emission lines give an incomplete assay of the chemical properties of the region. We can only measure abundances in the gas phase, and have no simple way to estimate the fraction of elements locked up in dust grains. Indeed, the depletion factors quoted implicitly assume that the solar abundance values (relative to H) are relevant, an assumption at least borne out by observations of the abundances of the undepleted species.

An example of where dust depletion must be taken into account is in the modeling the properties of HII regions and PNe. Sophisticated nebular models now routinely include consideration of the depletion of gas-phase abundances due to dust grains. They do this empirically as there is as yet no a priori way to estimate depletions from first principles. An additional complication of such models is that as dust grains are destroyed (e.g., by shocks or photoevaporation by UV photons), they will return otherwise depleted elements into the gas-phase. For refractory species like Fe and Ca that are strongly depleted onto grains, this can have serious implications for interpreting their nebular lines.

Implications for grain composition

Studies of the most abundant products of stellar nucleosynthesis (C, N, O, Mg, Si, S, and Fe) tell us about the primary constituents of grains. Elements formed by the r- and s-process are rarer, but may hold clues as to how the elements are processed through grains (either the incorporation or release of atoms from grains).

Oxygen:

Depending on the assumed (O/H) total abundance, something like 120–450 oxygen atoms per 10^6 H atoms reside in dust grains. The general absence of the $3.1\mu\text{m}$ H_2O band suggests that $<0.02\%$ of this Oxygen is locked up in H_2O ice. The rest is probably incorporated into silicates and oxides of Fe and Mg.

Carbon:

The C/H abundance in dust ranges from ~ 90 – 130 per 10^6 H atoms. This is small compared to the carbon content of dust grains inferred by the MRN or Draine & Lee dust mixtures.

Nitrogen & Sulfur:

These show little or no incorporation into dust grains.

Mg, Fe, Si, Ni, Cr, & Mn:

All of these elements show a high degree of incorporation into dust grains, in many cases nearly depleting the gas phase in favor of grains in dusty regions.

Rare elements:

Many have $(X/H)_{\text{gr}} \approx 70\% (X/H)_{\text{ISM}}$, but a few, notably P, Cl, As, Ar, Se, Kr, Sn, and Tl, show little or no incorporation into grains.

The problem of Carbon, one of the most abundant α -process elements, is such that there is often talk of a “carbon crisis” in the ISM. The observed total C abundances are about 0.2dex below Solar for B stars (the best source of total C abundances because no dust can survive in a B-star atmosphere). Given the observed gas-phase abundances, the implication is that there is less C available than is needed by typical dust mixtures to explain the strengths of features in the interstellar extinction curve due to carbonates. The problem is especially acute for the 2175\AA bump in the UV, which requires much larger carbon abundances than observed. The “crisis”, so far unresolved, can be summarized as “Where is all the Carbon we (think we) need for interstellar dust?”